

Thermal and X-ray analysis of racemic bupivacaine hydrochloride

A. Sykuła-Zajac · E. Łodyga-Chruścińska ·
B. Pałecz · R. E. Dinnebier · U. J. Griesser ·
V. Niederwanger

Received: 25 August 2010 / Accepted: 23 February 2011 / Published online: 26 March 2011
© The Author(s) 2011. This article is published with open access at Springerlink.com

Abstract An amide-type local anesthetic drug, bupivacaine hydrochloride (BupiHCl), in the form of racemate is listed in the European and American pharmacopoeias and continues to be used in medicine. Thermal and X-ray analysis of commercial BupiHCl monohydrate was performed by differential scanning calorimetry with thermogravimetry, hot stage microscopy, and X-ray diffraction. Endothermic dehydration occurs at the temperature range of 73–130 °C for DSC–TG 111 (Setaram) and at 83–150 °C for DSC 404 (Netzsch). Both curves at 2 and 10 °C min⁻¹ clearly reflect phase transformation of anhydrous Form I into II before reaching the melting point. A well-defined exothermic phase transition of BupiHCl was detected at a lower heating rate. Temperature-resolved X-ray diffraction in conjunction with DSC led to determining a similarity between the obtained thermal events. Microscopic investigation also confirmed the above-mentioned transformations.

Keywords Local anesthetics · Bupivacaine hydrochloride · Racemate · Thermal analysis · X-ray diffraction

Introduction

Bupivacaine hydrochloride (BupiHCl) is a long-acting local anesthetic widely used in clinical practice. This water-soluble compound is listed in the European and American pharmacopoeias. Bupivacaine is a xylylidine derivative which belongs to the family of 1-alkyl-2',6'-pipecoloxylidides (Fig. 1) which is promising in terms of reversibly blocking potential action in sensory nerves by means of a receptor-independent mechanism [1]. The administration of local anesthetics in the form of a free base or in the ionized state can induce analgesia either by general physicochemical disturbance of the neuron myelin sheath or by closing ionic sodium channels in the neuronal membrane [2].

The drug is still clinically available as a racemate which consists of “left-handed” *S*(-)- and “right-handed” *R*(+)-[3] enantiomers at a ratio of 50:50 [4]. *S*(-)-bupivacaine, which is called levobupivacaine [5, 6] produces a neuronal blockade of a longer duration and is less toxic to the central nervous and cardiovascular systems [7, 8]. Therefore, more and more studies concerning levobupivacaine have been reported in the literature [9–13]. Nevertheless, racemic mixtures of bupivacaine are still in common use in medicine.

Commercial ‘as is’ bupivacaine hydrochloride was determined by Giron et al. [14] to be a monohydrate which transforms into an anhydrous form upon heating. They also showed the potential existence of solvates with ethanol, isopropanol, and ethyl acetate. BupiHCl in the form of

A. Sykuła-Zajac (✉) · E. Łodyga-Chruścińska
Institute of General Food Chemistry, Faculty of Biotechnology
and Food Sciences, Technical University of Lodz,
Stefanowskiego 4/10, 90-924 Lodz, Poland
e-mail: anna.sykula-zajac@p.lodz.pl

B. Pałecz
Department of Physical Chemistry, Faculty of Physics
and Chemistry, University of Lodz, Pomorska 149/153,
90-236 Lodz, Poland

R. E. Dinnebier
Max Planck Institute for Solid State Research, Heisenbergstrasse
1, 70569 Stuttgart, Germany

U. J. Griesser · V. Niederwanger
Department of Pharmaceutical Technology,
Institute of Pharmacy, Leopold Franzens University Innsbruck,
Innrain 52, 6020 Innsbruck, Austria

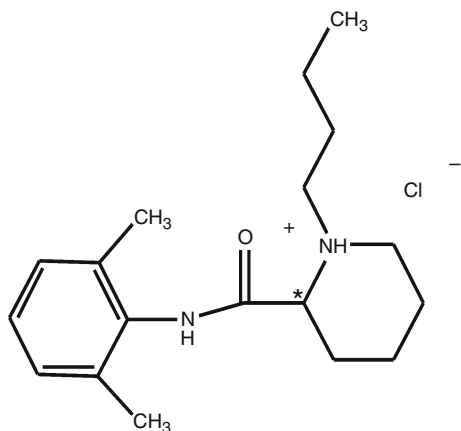


Fig. 1 Molecular formula of bupivacaine hydrochloride ($C_{18}H_{28}N_2 \cdot O \cdot HCl, H_2O, 342.99 \text{ g mol}^{-1}$)

monohydrate is not very stable thermally and dehydrates at above $60 \text{ }^\circ\text{C}$.

Statistical analyses show that only about 10% of racemates are conglomerates, while the vast majority of them are racemic compounds. Bupivacaine belongs to that 10% group of conglomerate compounds, which offers the possibility for optical resolution by preferential crystallization [15].

Moreover, it is known that Bupivacaine HCl is polymorphic [16]. Temperature-resolved X-ray experiments performed by Giron et al. demonstrated the existence of two anhydrous forms. The forms were detected by heating and cooling processes fluctuating between 100 and $170 \text{ }^\circ\text{C}$ [14]. Furthermore, four new forms of Bupivacaine HCl were discovered by utilization of the “Basic Screen” polymorph screening protocol and were differentiated using instrumental methods such as differential scanning calorimetry (DSC), X-ray powder diffraction (XRPD), and polarized light microscopy (PLM).

The present thermal and X-ray analysis was performed on the currently most popular racemic mixture of Bupivacaine HCl. The objective of this study was to carefully investigate the thermal behavior of the widely administered drug using thermal analytical techniques (DSC, TGA, and thermomicroscopy) and X-ray diffractometry to identify any relationships between the obtained results.

Experimental

Material

Bupivacaine HCl was purchased as a monohydrate from Sigma-Aldrich, Inc., St. Louis, United States of America (99% purity). The commercial substance occurs in the form of white crystal powder.

Thermal investigations

Thermal investigations were performed by DSC 404 (Netzsch, Selb) using the TA Universal Analysis software. A Sartorius balance was used to weigh a $4.4 \pm 0.0005 \text{ mg}$ sample into an aluminum pan (Perkin-Elmer) with a perforated cover. Dry argon was used as the purge gas (purge: 75 mL min^{-1}), and the system was calibrated with indium (purity 99.999%, melting point $156.6 \text{ }^\circ\text{C}$, heat of fusion 28.60 J g^{-1}), tin (melting point $232.70 \text{ }^\circ\text{C}$, heat of fusion 60.40 J g^{-1}), and quartz (melting point $573.50 \text{ }^\circ\text{C}$, heat of fusion 8.40 J g^{-1}). A heating rate of $10 \text{ }^\circ\text{C min}^{-1}$ was routinely used.

A differential scanning calorimeter coupled with a Setaram DSC–TG 111 thermobalance was also used in thermal investigations. A $6.21 \pm 0.0005 \text{ mg}$ sample was weighed into an aluminum pan using a Mettler AE20 balance. Dry nitrogen was used as the purge gas (purge: $30\text{--}40 \text{ mL min}^{-1}$), and the system was calibrated with indium (purity 99.999%, melting point $156.6 \text{ }^\circ\text{C}$, heat of fusion 28.45 J g^{-1}), lead (melting point $327.50 \text{ }^\circ\text{C}$, heat of fusion 23.22 J g^{-1}), zinc (melting point $419.47 \text{ }^\circ\text{C}$, heat of fusion 103.79 J g^{-1}), and tin (melting point $231.93 \text{ }^\circ\text{C}$, heat of fusion 60.60 J g^{-1}). A heating rate of $2 \text{ }^\circ\text{C min}^{-1}$ was routinely used.

The thermal behavior of the solid-state forms was examined with a Reichert Thermovar[®] polarization microscope (Reichert, Vienna, A) equipped with a Kofler hot stage (Reichert, Vienna, A). Microphotographs were produced with $200 \text{ }\mu\text{m}$ scale bars.

Temperature-resolved XRPD investigations

Structural investigations were performed at the Angströmquelle Karlsruhe (ANKA) synchrotron in Karlsruhe, at the Max Planck Institute. The source of radiation at the beamline was a 1.5 T bending magnet, which offered X-ray energies between 6 and 20 keV . The first optical device in the path of X-rays was a rhodium-coated silicon mirror. The mirror focused the beam in the vertical direction. A double silicon (111) crystal monochromator was used to select the wavelength of 1.238879 \AA and focus the beam in the horizontal direction [17]. The measurement was done in Debye–Scherrer mode with the sample spun to improve counting statistics. A MarCCD 165 detector was used for the detection of scattered peak intensities. A modified Leister 700 hot air tool with a tubular nozzle was used as a heating device. The temperature was controlled by a Eurotherm 2461 self-optimizing temperature controller. The hot air blower was set vertically several millimeters below the capillary. The pin was fitted into a Huber goniometer head and aligned. The measurements were performed at a $35\text{--}305 \text{ }^\circ\text{C}$ temperature range with a

dynamic mode of heating rate close to $1.5\text{ }^{\circ}\text{C min}^{-1}$. The whole time of measurement totalled 3 h. Treatment of the X-ray powder patterns obtained was done with Powder3D [18].

Results and discussions

Thermal investigations of racemic BupiHCl

Thermal investigations using DSC

The thermal curves obtained from two calorimeters, one of which was equipped with a thermobalance, are presented in Fig. 2. The first, standard measurement of the commercial mixture was done with a DSC 404 calorimeter using only the DSC method at $10\text{ }^{\circ}\text{C min}^{-1}$ at the Max Planck Institute in Stuttgart. Double heating without TG measurement or cooling of the BupiHCl sample was performed (gray solid and dotted lines, respectively). The DSC curve of the first heating is similar to the curve obtained by Giron et al. [14]. The Netzsch Thermal Analysis software was used to determine the temperatures of the peaks. The corresponding endothermic peaks at 116.60 and $133.40\text{ }^{\circ}\text{C}$ ($E_{\text{endo}} = 191.8\text{ mW}$) probably present a two-stage dehydration process. The temperature range of the dehydration process is rather wide; therefore, a deconvolution operation was performed. The deconvolution of coupled peaks was done with the PeakSeparation (PeakSep) software (Netzsch). The onset and endpoint of the first peak are at 111.60 and $124.00\text{ }^{\circ}\text{C}$, respectively. The second step of the dehydration process of BupiHCl starts at $113.50\text{ }^{\circ}\text{C}$ and ends at $142\text{ }^{\circ}\text{C}$. The percentage area of the corresponding peaks was calculated. The percentage values of the areas

are *ca.* 21 and 79%, respectively. Hence, one can suppose that the release of water molecules during dehydration takes place at the ratio of 1 to 4. Probably two-stage dehydration was observed, because the decomposition of hydrates (including solvates) is supposed to occur by progressive evacuation of the solvent through interlayer planes or channels controlled by an overall diffusion process [19].

Exothermic phase transition was observed at above $150\text{ }^{\circ}\text{C}$ (after the dehydration process) on the DSC curve at $10\text{ }^{\circ}\text{C min}^{-1}$. The transition starts and ends at 170.80 and $210\text{ }^{\circ}\text{C}$, respectively (see inset in Fig. 2). The phase transition ($E_{\text{exo}} = -5.2\text{ mW}$) probably corresponds to the change of the metastable form (Form I) of the anhydrate existing in the range $150\text{--}170\text{ }^{\circ}\text{C}$ into the stable form (Form II) present in the temperature range of $210\text{--}240\text{ }^{\circ}\text{C}$. Form II is monotropically related to Form I as it was observed in the corresponding temperature range for exothermic transition on the first and second heating curves shown in Fig. 2 (dotted line). Form II exists up to the decomposition process of the sample at $\sim 240\text{ }^{\circ}\text{C}$. Above this temperature, the BupiHCl sample undergoes decomposition as shown by the second heating curve. A second heating does not reveal any thermal event throughout the temperature range. Therefore, a second heating was not applied in subsequent measurements.

Thermal investigations using DSC–TG 111

BupiHCl was reexamined using the DSC–TG method at $2\text{ }^{\circ}\text{C min}^{-1}$ at a temperature range of $20\text{--}203\text{ }^{\circ}\text{C}$ to investigate it using another calorimeter equipped with a thermobalance and at a lower heating rate. Measurement at higher temperatures was not performed due to the risk of contamination of the thermobalance.

The DSC curve at $2\text{ }^{\circ}\text{C min}^{-1}$ reveals the suggested two-stage dehydration process and a well-defined exothermic phase transition (Fig. 2). Both curves at 2 and $10\text{ }^{\circ}\text{C min}^{-1}$ clearly and consistently reflect phase transformation of the anhydrous substance before the melting point. Due to a slower heating rate, the corresponding temperatures of 109.97 and $117.178\text{ }^{\circ}\text{C}$ ($E_{\text{endo}} = 167.2\text{ mW}$) in the dehydration and phase transition of the anhydrous form ($178.16\text{ }^{\circ}\text{C}$, $E_{\text{exo}} = -4.7\text{ mW}$) begin earlier than observed on the DSC curve obtained with the Netzsch instrument. The anhydrous Form I exists between 130 and $163\text{ }^{\circ}\text{C}$ and the anhydrous Form II from $194\text{ }^{\circ}\text{C}$ to the decomposition of the sample.

The use of a thermobalance in the analysis enabled estimating the loss of mass during thermal dehydration. No two-stage dehydration process was observed on the TG curve, as opposed to both DSC curves. It is probably due to the gradual release of water molecules from the racemic crystals of BupiHCl. During dehydration alone mass

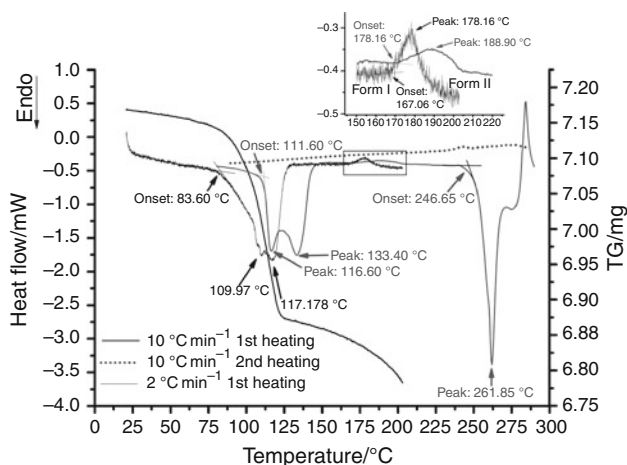


Fig. 2 Thermal curves of racemic bupivacaine hydrochloride at $2\text{ }^{\circ}\text{C min}^{-1}$, first heating (DSC–TG 111), and at $10\text{ }^{\circ}\text{C min}^{-1}$, first and second heating (DSC 404); the inset shows the range of exothermic transition

variation was 0.277 mg. Furthermore, the ratio of water molecules in BupiHCl equals 1:1.186 and confirms that the commercial substance has the monohydrate form.

Thermomicroscopic investigations

The thermomicroscopic behavior of racemic BupiHCl crystals using hot stage microscopy at a heating rate of 5–10 C min⁻¹ (HTM) is given in Fig. 3. BupiHCl monohydrate crystals at 25 °C occur as small and large particles not exceeding 200 μm (Fig. 3a).

Parallel cracks form in crystals under the influence of temperature (Fig. 3b, see yellow arrow), but at the same time the initial shape of the crystals is maintained. The cracks are the result of dehydration of the substance. The thermal process probably happens because of gradual release of water from interlayer planes or channels. Reorganization begins in the inner part of each particle without loss of crystallinity [19, 20]. Heated crystals undergo chemical degradation, which was confirmed by the darkening of crystals. This phenomenon was also noticed by Kuhnert-Brandstätter [21] during analysis of BupiHCl monohydrate. The tested substance transformed into anhydrous form at 115 °C with a simultaneous darkening of the crystals.

After the dehydration process, the appearance of new crystalline forms (Fig. 3c and d) was detected in the temperature range of 135–190 °C. While heating, they exhibit further growth and nucleation. The newly obtained crystalline forms (Fig. 3d) occur as long, narrow, and blunt-ended crystals. “Nucleation and growth” models assume that transitions start at a particular site (generally, crystal

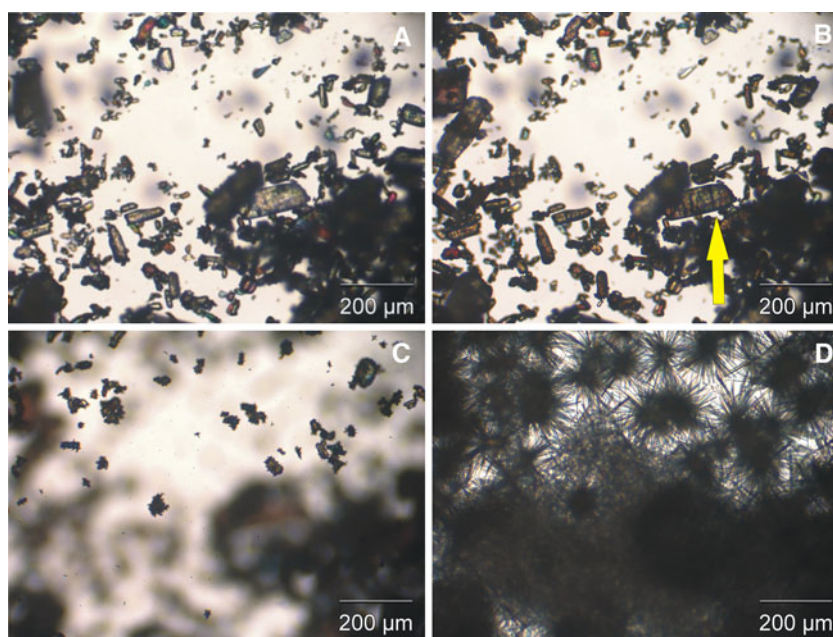
defects for polymorphic transitions and particle surface for dehydrations) and continue by a progressive propagation of the reaction interface [19]. The expected polymorphic transition between the anhydrous Forms I and II proceeds by nucleation and growth.

Temperature-resolved X-ray and DSC investigations

The thermal behavior of BupiHCl was compared with DSC results and temperature-resolved X-ray diffraction data. The X-ray patterns of BupiHCl monohydrate were identified using the ANKA synchrotron. The patterns in the 3D project were analyzed against the DSC curves obtained with a Setaram DSC–TG 111 calorimeter (Fig. 4). The XRD patterns and the DSC curve were both recorded at a very similar heating rate.

Endothermic dehydration and exothermic phase transition measured at corresponding temperatures observed on the DSC curve also appeared in the collection of 3D-plot X-ray patterns. The existence of an exothermic event in the X-ray pattern set has not been reported so far. The above-mentioned processes are shifted in terms of temperature. In addition, Fig. 5 shows approximately the corresponding X-ray patterns of exothermic phase transition for anhydrous BupiHCl. The data present the temperature values from the DSC curve (DSC–TG 111) and the counting time at each temperature for corresponding X-ray patterns. Moreover, in Fig. 5 the temperature values of exothermic transition occurring in the X-ray pattern set were added as red arrows. The temperatures, which demonstrate an onset (163 °C), peak point (178.16 °C), and endpoint (194 °C) of exothermic phase transition, do not overlap with the X-ray

Fig. 3 Microphotographs of racemic bupivacaine hydrochloride monohydrate at **a** 25 °C, **b** 110 °C, **c** 135 °C, and **d** 190 °C



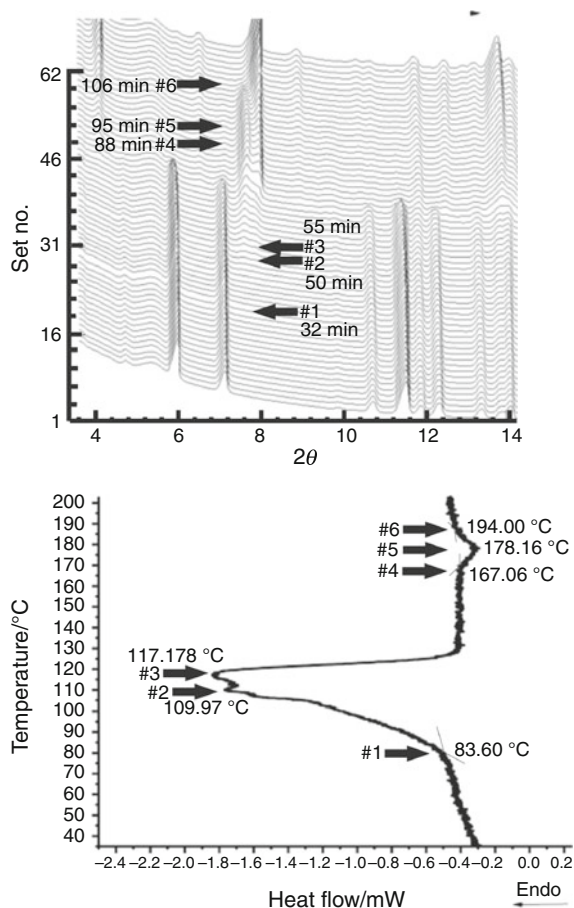


Fig. 4 3D X-ray patterns and the DSC curve at the temperature range of 35–203 °C for BupiHCl monohydrate showing both the endothermic process of dehydration and exothermic phase transition. The data show the exact temperature values of DSC thermal events and the counting time at each temperature for respective X-ray patterns

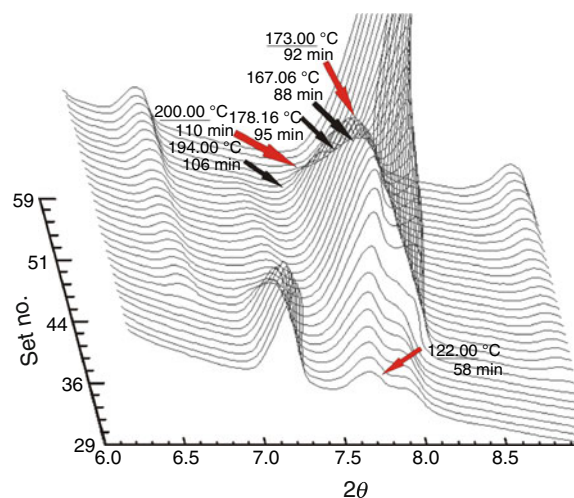


Fig. 5 3D X-ray patterns showing exothermic phase transition approximately [the corresponding temperatures occurring on the DSC curve (DSC–TG 111) and temperature values with counting time at each temperature for respective X-ray patterns]

patterns exactly. Probably Forms I and II exist at the same temperature range simultaneously.

Conclusions

The commercial form of racemic BupiHCl, being a monohydrate, transforms into the anhydrous form which undergoes further transformation (Form I → Form II) during heating. All of the methods used, i.e., DSC with thermogravimetry, hot stage microscopy, and X-ray diffraction confirm the presence of endothermic dehydration and exothermic phase transition of BupiHCl.

No two-stage dehydration process was observed on the TG curve, in contrast to both DSC curves. It is probably due to the gradual release of water molecules from BupiHCl racemic crystals. During dehydration, mass variation was 0.277 mg. The ratio of water molecules in BupiHCl equals 1:1.186, which confirms the claim that the commercial substance occurs in monohydrate form.

Phase transition is detected after BupiHCl dehydration. Furthermore, both DSC curves obtained from different calorimeters at the heating rates of 2 and 10 °C min⁻¹ clearly reflect the phase transformation of the anhydrous substance before the melting point.

DSC and X-ray diffraction are two powerful tools in studying the thermal behavior of racemic BupiHCl. DSC alone cannot perfectly detect phase transitions of very low enthalpies. On the other hand, X-ray diffraction is unable to provide thermodynamic information relating to phase transition. In the course of using the conventional method, more problems will arise from the thermal history of the sample. Thus, the best solution is to apply both techniques. In our case, the comparison of evidence of exothermic phase transition seen both in X-ray diffraction patterns and the DSC curve was possible at almost the same heating rate (1.5–2 °C min⁻¹). The respective temperatures reflected in the DSC curve (DSC–TG 111), which demonstrate the onset (163 °C), peak point (178.16 °C), and endpoint (194 °C) of the exothermic phase transition, do not overlap with the X-ray patterns exactly. Probably Forms I and II exist at the same temperature range simultaneously.

Thermomicroscopic analysis shows parallel cracks resulting from the dehydration of the substance. Furthermore, upon heating crystals undergo chemical degradation, confirmed by their darkening. Subsequently, new anhydrous crystalline forms are obtained in the temperature range of 135–190 °C. Thermomicroscopic analysis confirms the thermal transformation of BupiHCl racemate.

Acknowledgements Marek Zakrzewski, PhD of Analytics Sp. z o.o. is acknowledged for a helpful discussion and an investigative engagement in the area of solid state characterization of

pharmaceuticals. This study was supported under a “Mechanizm WIDDOK” scientific project (contract number WIDDOK/SC/2007/28) by the European Social Fund and the Republic of Poland.

Open Access This article is distributed under the terms of the Creative Commons Attribution Noncommercial License which permits any noncommercial use, distribution, and reproduction in any medium, provided the original author(s) and source are credited.

References

1. Csöregi I. Structures and absolute configurations of enantiomers of two local anaesthetics: (2*S*)-1-methyl- and (2*R*)-1-butyl-2',6'-pipecoloxylidide hydrochlorides. *Acta Crystallogr Sect C Cryst Struct Commun.* 1992;C48:1794–8.
2. Cheung EY, Harris KDM, Johnston RL, Kitchin SJ, Hadden KL, Zakrzewski M. Rationalizing the structural properties of bupivacaine base—a local anesthetic—directly from powder X-ray diffraction data. *J Pharm Sci.* 2004;93:667–74.
3. Palkama VJ, Neuvonen PJ, Olkkola KT. Effect of itraconazole on the pharmacokinetics of bupivacaine enantiomers in healthy volunteers. *Br J Anaesth.* 1999;83:659–61.
4. Cox CR, Faccenda KA, Gilhooly C, Bannister J, Scott NB, Morrison LMM. Extradural *S*(-)-bupivacaine: comparison with racemic *RS*-bupivacaine. *Br J Anaesth.* 1998;80:289–93.
5. Foster RH, Markham A. Levobupivacaine: a review of its pharmacology and use as a local anaesthetic. *Drugs.* 2000;59:551–79.
6. McLeod GA, Burke D. Levobupivacaine. *Anaesthesia.* 2001;56:331–41.
7. Gristwood RW. Cardiac and CNS toxicity of levobupivacaine: strengths of evidence for advantage over bupivacaine. *Drug Saf.* 2002;25:153–63.
8. Huang YF, Pryor ME, Mather LE, Veering BT. Cardiovascular and central nervous system effects of intravenous levobupivacaine and bupivacaine in sheep. *Anesth Analg.* 1998;86:797–804.
9. Mather LE, Huang YF, Veering B, Pryor ME. Systemic and regional pharmacokinetics of levobupivacaine and bupivacaine enantiomers in sheep. *Anesth Analg.* 1998;86:805–11.
10. Langston M, Dyer UC, Frampton GAC, Hutton G, Lock CJ, Skead BM, Woods M, Zavareh HS. Racemisation of R-bupivacaine: a key factor in the integrated and economic process for the production of levobupivacaine. *Org Process Res Dev.* 2000;4:530–3.
11. Fawcett JP, Kennedy JM, Kumar A, Ledger R, Kumara GM, Patel MJ, Zacharias M. Comparative efficacy and pharmacokinetics of racemic bupivacaine and *S*-bupivacaine in third molar surgery. *J Pharm Pharm Sci.* 2002;5:199–204.
12. Frawley GP, Downie S, Huang GH. Levobupivacaine caudal anesthesia in children: a randomized double-blind comparison with bupivacaine. *Pediatr Anesth.* 2006;16:754–60.
13. Erdil F, Bulut S, Demirbilek S, Gedik E, Gulhas N, Ersoy MO. The effects of intrathecal levobupivacaine and bupivacaine in the elderly. *Anaesthesia.* 2009;64:942–6.
14. Giron D, Draghi M, Goldbronn C, Pfeffer S, Piechon P. Study of the polymorphic behaviour of some local anesthetic drugs. *J Therm Anal.* 1997;49:913–27.
15. Nemák K, Ács M, Kozma D, Fogassy E. Racemic compound formation-conglomerate formation. Part 4. Optical resolution and determination of the melting phase diagrams of 2',6'-pipecoloxylidide and four 1-alkyl-2',6'-pipecoloxylidides. *J Therm Anal.* 1997;48:691–6.
16. Łodyga-Chruścińska E, Zakrzewski M, Kuberski S, Paluszkiwicz A, Dinnebier RE, Sugimoto K. Preliminary characterization of new polymorphic forms of bupivacaine HCl. *Ann Pol Chem Soc.* 2005;2:87–90.
17. Heinrich J editor. Anka Angstroemquelle Karlsruhe, Anka-Instrumentation book. ISS Institute for synchrotron radiation; 2007.
18. Hinrichsen B, Dinnebier RE, Jansen M. Powder3D: an easy to use programme for data reduction and graphical presentation of large numbers of powder diffraction patterns. *Z Kristallogr.* 2006;23:231–6.
19. Petit S, Coquerel G. Mechanism of several solid-solid transformations between dihydrated and anhydrous copper(II) 8-hydroxyquinolinates. Proposition for a unified model for the dehydration of molecular crystals. *Chem Mater.* 1996;8:2247–58.
20. Galwey AK. Some recent studies of the mechanisms of dehydration reactions of solids. *J Therm Anal.* 1992;38:99–110.
21. Kuhnert-Brandstätter M, Kofler A, Kramer G. Beitrag zur mikroskopischen charakterisierung und identifizierung von arzneimitteln unter einbeziehung der UV-spektrophotometrie. *Sci Pharm.* 1974;42:150–63.